International Journal of Engineering and Allied Sciences (IJEAS)
||Volume 1|| ||Issue 1|| ||2015||

DFT study of electronic, mechanical and optical properties of Zn-chalcogenides

Manoj Kausik

Department of Chemistry, Sanjay Institute of Engineering and Management, Mathura
Uttar pradesh, India
piuks@rediffmail.com

----------ABSTRACT----------

With the Density Functional Theory, full potential linearized-augmented plane-wave plus local orbitals (FP-LAPW+l0) method within the generalized gradient approximation (GGA) is used to calculate the electronic, elastic and linear optical properties of Zn-chalcogenides ZnX (X= S, Se, Te) compounds. Elastic properties calculation shows the ductile nature of the Zn-chalcogenides. The linear optical properties such as dielectric function, electron energy-loss, and refractive index are obtained. In the plots of the imaginary part of the complex dielectric function, the absorption threshold shifts toward lower energy with the increase in chalcogen atomic number.

Keywords *- **Density Functional Theory; FP-LAPW+l0; Zn-chalcogenides; Optical properties; Dielectric function.***

I. INTRODUCTION

Binary chalcogenides ZnX with X= S, Se, and Te are prototype II-VI semiconductors. These compounds with zinc-blende (ZB) structures, and isotropic optical properties are potential candidate for the optical device technology. They are used in visual displays, high-density optical memories, transparent conductors, solid-state laser devices, solar cells, etc. It is very important to get in-depth knowledge about optical properties of these materials, especially in the design of ZnX-based optoelectronic devices. Optical properties of ZnX compounds have extensively been studied in the past [1-6]. A detailed systematic survey on optical parameters for Zn chalcogenides is available in the literature [7]. There is inconsistency between some of the experimental values for the optical parameters. For example Klucker et al [8] found the peak in the spectra of imaginary part of the dielectric function and reflectivity corresponding to the fundamental absorption edge, whereas the same was found to exist in the energy range 10–15 eV in another experimental result [7].

Many reports on the theoretical work for optical properties calculations are available. Density functional theory [9] (DFT) in the local-density approximation [10] (LDA) has been used for the optical properties calculation for ZnX binary compound. The optical spectra have been investigated [11] by solving the Bethe- Salpeter equation. Full potential linearized augmented plane-wave method plus local orbitals (FP-LAPW+l0) within the generalized gradient approximation (GGA) and LDA has been used for band structure calculations. FP-LAPW+l0 is very efficient method to identify not only the energy location of the Zn 3d electrons and associated band parameters [12, 13], but also to address the optical response. The ab initio full potential with linear muffin-tin orbital methods within LDA [14, 15] and the projector-augmented wave (PAW) method within both of LDA and GGA [12, 13] have been used for the calculation of electronic properties of ZnO wurzite structure. But the order of states at the top of the valence band (VB), the location of the Zn 3d band and its width do not agree well with other calculated values [12-15]. It is clear that there exist a number of calculations for the electronic and optical properties determination using different methods, but very few full potential

calculations exist for these compounds. From literature survey, it can be seen that the calculated energy gaps vary from 2.3 to 3.8 eV for ZnS, 1.6 to 2.8 eV for ZnSe and 1.4 to 2.4 eV for ZnTe. The experimental result shows the energy gaps [16] as 3.8 eV for ZnS, 2.8 eV for ZnSe and 2.4 eV for ZnTe.

The large variation in the energy gap values reveals the dependence on the method of the band structure calculation. On the other hand some calculated energy gaps are in good agreement with the measured energy gaps, which is unlikely from calculations based on the local density approximation. Keeping it in mind, we perform calculations using the full potential linear augmented plane wave plus local orbitals (FP-LAPW+l0) method.

The aim of this work is to give a detailed description of the behavior of electronic, elastic and linear optical properties of ZnX compounds. We have used FP-LAPW+l0 method in order to re-investigate properties and compare the results with experimental and theoretical works on these compounds.

II. COMPUTATIONAL DETAILS

The elastic, electronic, and optical properties of ZnX chalcogenides have been estimated in the frame work of density functional theory [9]. The full potential linearized augmented plane wave plus local orbitals (FP-LAPW + lo) approach with Wien2k code [17, 18] has been used for calculations. The present work considers the generalized gradient approximation (GGA) with Perdew, Burke and Ernzerhof (PBE) parameter to elucidate the exchange and correlation effects [19]. ZnX compounds exist in the zinc-blende structure of space group F-43 m. We placed Zn atom at the position (0, 0, 0) while placing X atom at position (0.25, 0.25, 0.25). Furthermore Murnaghan's equation of state [20] is employed to optimize the total energy as a function of the volume of the unit cell. Through the minimization of energy we estimate the equilibrium structural parameter, viz., cell dimension and geometry. The present calculation considered the value of RMTkmax as 7, so that it can attain the convergence over energy eigen value. It is worthy to be mentioned that RMT is the least radius of the muffin-tin (MT) spheres. kmax represents maximum value of the wave vector. We have taken the values of muffin-tin radii (RMT) for Zn, S, Se and Te as 2.2, 2.1, 2.3 and 2.6 a.u. (atomic units) respectively for entire calculation. With the value of the angular momentum with maximization, denoted as lmax as 10 the wave function is made extended inside the spheres of atom. Monkhorst–Pack k-points [21] of matrix size 10×10×10 is used to construct the irreducible Brillouin zone (BZ) for the zinc-blende structure. An iteration procedure is followed to reach the convergence of total energy and charge well below 0.0001Ry and 0.001e, respectively.

III. RESULTS AND DISCUSSIONS

Structural and elastic properties

We fitted the Murnaghan's equation of state [20] in the plot of the total energy versus unit cell volume to estimate different parameters, for example, the equilibrium lattice dimension (a_0), bulk modulus B_0, the pressure derivative of the bulk modulus B_0'. Table 1 represents the calculated values of a_0, B_0 and B_0' for ZnX in the ZB structure at equilibrium. ZnS has the equilibrium lattice parameter $a_0 = 5.369$, ZnSe shows its equilibrium lattice parameter at $a_0 = 5.629$. ZnTe has the value of a_0 as 6.191. All these calculated values agree well with the experimental values as reflected in the table 1. The maximal error is determined as of 1.51% in comparison to experimental values. It sounds understandable

that well-defined structural properties are supportive for additional revision of electronic and optical properties.

Table 1: Calculated lattice constant (in A°), bulk modulus B_0 (in GPa), pressure derivative B_0' for ZnX compounds compared to experimental works.

	a_0	B_0	B_0'
ZnS			
Present	5.371	90.12	4.32
Expt.	5.412[a]	75[a]	4.00[a]
ZnSe			
Present	5.632	72.42	4.76
Expt.	5.667[b]	69.3[b]	
ZnTe			
Present	6.198	60.39	4.71
Expt.	6.103[c]	50.9[c]	5.04[c]

[a] Ref. [2], [b]Ref. [3], [c]Ref. [4].

We used WIEN2k code with Charpin method [22] to calculate the elastic constants of ZnX compounds existing in the cubic structure. In this method appropriate lattice distortions are applied for the perturbing the cubic lattice. Subsequently the distorted lattice is used for the determination of the independent elastic constants C_{11}, C_{12}, and C_{44}. The following three equations are considered for the calculation of the elastic constants.

$$B_0 = (C_{11} + 2C_{12})/3 \tag{1}$$

$$\Delta E_{rhomb} = \frac{1}{6}(C_{11} + 2C_{12} + 4C_{44})V_0\delta^2 \tag{2}$$

$$\Delta E_{tetra} = 6(C_{11} - C_{12})V_0\delta^2 \tag{3}$$

The value of B_0 as calculated from Murnaghan's equation is put in the first equation which establishes the relation of the bulk modulus B_0 with the elastic constants (C_{11} and C_{12}). The variation of strain energy (ΔE_{rhomb}) with volume-conserving rhombohedral strain (δ) is represented in the second equation. A relation of strain energy (ΔE_{tetra}) with the volume conserving tetragonal strain (δ) is represented in the third equation. Using these three equations we have calculated the elastic constants for the zinc-blende structured ZnX as exhibited in Table 2 along with comparison of the calculated values with experimental result [23]. Calculated values showed a good agreement with the obtainable experimental data.

Table-2: Calculated values of elastic constants (C_{ij} in GPa) at equilibrium for ZnX compound.

	C_{11}	C_{12}	C_{44}
ZnS			
Present	111	71	69
Expt.[a]	104	65	46.2
ZnSe			
Present	91	63	59
Expt.[a]	85.9	50.6	40.6
ZnTe			
Present	79	48	41
Expt.[a]	71.7	40.7	31.2

[a] Ref. [23]

It is observed that the elastic constants decline in magnitude with increase in lattice parameter when one goes from S to Te. It is explained by the fact that cohesive energy reduces with the nearest neighbour distance [24]. It is well known that a cubic crystal retains the mechanical stability demanding the elastic constants maintain the following conditions:

$$C_{11} - C_{12} > 0, \quad C_{44} > 0, \; C_{11} + 2C_{12} > 0, \; C_{12} < B_0 < C_{11}.$$

The condition for mechanical stability is well maintained as depicted in Table 2. Further calculated values of the elastic constants namely C_{11}, C_{12} and C_{44}, have been utilised to estimate Bulk modulus (B_0), Young's modulus (Y) , Isotropic shear modulus (G) and Poisson ratio (σ) with the help of the following explicit expressions [25, 26],

$$G = (G_V + G_R)/2 \tag{4}$$

The value of G is the average of Voigt's shear modulus (GV) and Reuss's shear modulus (GR) for cubic crystals. The expressions for G_V and G_R are given by:

$$G_V = \frac{C_{11} - C_{12} + 3C_{44}}{5} \tag{5}$$

$$G_R = \frac{5C_{44}\left(C_{11} - C_{12}\right)}{4C_{44} + 3\left(C_{11} - C_{12}\right)} \tag{6}$$

Other two modulus namely, Young's modulus (Y) and Poisson's ratio (σ) are given by

$$Y = \frac{9GB}{G + 3B} \tag{7}$$

$$\sigma = \frac{3B - 2G}{6B + 2G} \tag{8}$$

Table 3 exhibits the calculated elastic modulus. Generally the bulk modulus B_0 is a measure of the resistance to fracture and the shear modulus G contributes as the resistance to plastic deformation.

Table-3: Calculated values of elastic modulus (in GPa)

	G (GPa)	B_0/G	C_{12}-C_{44} (GPa)	Y (GPa)	σ
ZnS	41.88662	2.15152	1.88	108.8	0.299
ZnSe	33.41409	2.16735	3.93	86.88	0.3
ZnTe	27.48057	2.19755	7.57	71.584	0.302

B_0/G ratio is an important parameter to understand the ductility of the material [27]. In the present work the B_0/G ratio for all ZnX are well above 1.75 (see Table 3). It tells about the ductile nature of Zn-chalcogenides compounds. It can be seen from the table that ZnTe bears the highest value of B_0/G ratio as 2.19 among all the ZnX compounds. It seems that ZnTe is the most ductile of all binary Zn-chalcogenides studied in the present work. There is a connection of the binding properties with ductility [28]. The well known Cauchy pressure (C_{12}–C_{44}) is correlated to the bond

character of the cubic compounds. More positive in the value of Cauchy pressure, compound is likely to form more profound metallic bond. Consequently, the ductile nature of the present ZnX compounds can be attributed to their positive Cauchy pressure which in turn ensures having the metallic character in their bonds. It can be depicted in Tabe 3 that the ZnTe possesses highest positive Cauchy pressure demonstrating strong metallic bonding (ductility) in comparison to other compounds.

Table 3 displays the value of Young's modulus (Y) as calculated in the present work. Young's modulus demonstrates the degree of stiffness of the solid; in a sense that more the stiffness, the material acquires the larger value of Y and at the same time such materials posseses covalent bonds. Table 3 demonstrates that the highest value of Y arises in ZnS, which is the attribute of more covalent in nature among the other ZnX compounds. Poisson's ratio (σ) is a measure of compressibility of solids. The values of σ for all present ZnX compounds exist between 0.29 and 0.30. It envisages that the Zn-chalcogenide compounds are compressible. A solid having the value of Poisson's ratio having in between 0.25 and 0.5 shows the bonding force more like as central force. In the present study, the Poisson's ratios of all binary chalcogenides are closed to 0.3, which tells that the bonding forces in the ZnX compounds are central in nature.

Calculation of Debye temperature

The Debye temperature (θD) is considered as a fundamental parameter for many physical properties of solids, such as specific heat, elastic constants, and melting temperature. At low temperature only the acoustic branches of phonons are active and the vibrational excitations take place exclusively from acoustic vibrations. Hence, the estimate of Debye temperature based on elastic constants at low temperature is consistent with the same as that determined from specific heat measurements. Once we have determined the elastic constants, we may obtain the Debye temperature (θD) by using the average sound velocity Vm by the equation, [29, 30]

$$\theta_D = \frac{h}{k_B}\left[\frac{3n}{4\pi}\left(\frac{N_A\rho}{M}\right)\right]^{1/3} V_m \tag{9}$$

Where h is Planck's constant, kB is Boltzmann's constant, n is the number of atoms per formula unit, NA is Avogadro's number, M is the molecular weight, ρ is the density. The average sound velocity (Vm) is given by [29, 31]

$$\mathrm{v_m} = \left[\frac{1}{3}\left(\frac{2}{\mathrm{v_t^3}} + \frac{1}{\mathrm{v_l^3}}\right)\right]^{-1/3} \tag{10}$$

Where vt and vl are the transverse and longitudinal sound velocities respectively given as follows

$$v_t = \sqrt{\frac{C_{44} - \frac{1}{5}\left(2C_{44} + C_{12} - C_{11}\right)}{\rho}} \tag{11}$$

$$v_l = \sqrt{\frac{C_{11} + \frac{2}{5}\left(2C_{44} + C_{12} - C_{11}\right)}{\rho}} \tag{12}$$

We have calculated density, the sound velocities and Debye temperatures by using the calculated elastic constants, which are given in Table 4.

Table 4: Calculated sound velocities and Debye temperatures for ZnX compounds

	ρ (Kg/m^3)	V_t (m/s)	V_l (m/s)	V_m (m/s)	θ_D (K)
ZnS	4110	3465	6041	3849	424
ZnSe	5260	2789	4908	3101	326
ZnTe	5650	2318	4178	2582	252

Electronic properties

We computed the electronic band structure of Zn chalcogenides. Figure 1 display the calculated structure for ZnS at equilibrium. ZnS is deliberated as a prototype; in the meantime the band structures are fairly alike for all three binary chalcogenides. The estimated band structure in the present work agrees very well with other theoretical results [36-39].

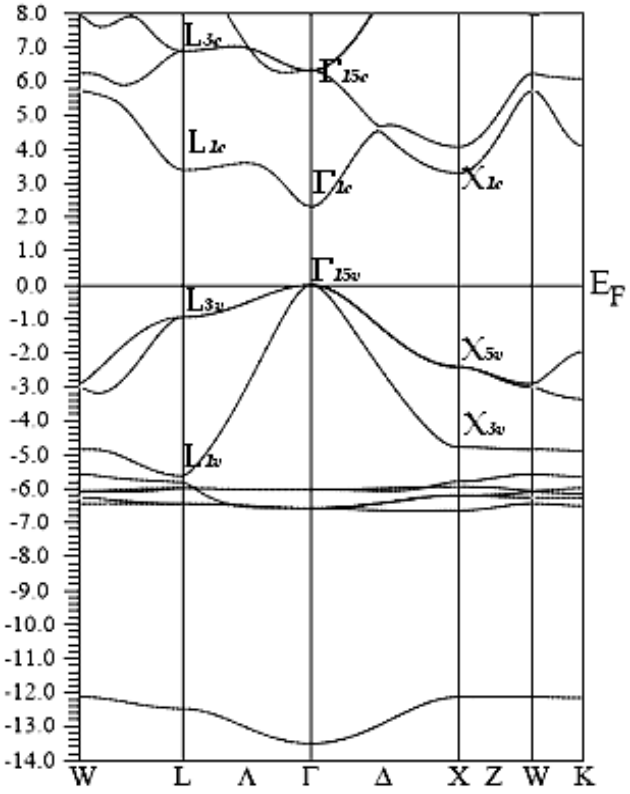

Figure 1: Electronic band structure for ZnS.

For convenience the top of the valence band (VB) is considered as the zero level of the energy scale. All the energy band structures are determined along the directions which contain high symmetry points in the first Brillouin zone, viz., W→ L→ Γ→ X→ W→K. Each of the ZnX compounds reveals the presence of the valence band maximum along with conduction band minimum

on the identical symmetry point. The appearances of band structures demonstrate the direct energy gap between the valence band and conduction band at Γ point. With the increase of the anion (X) atomic number in the Zn-chalcogenides, the X atom p bands move up in energy scale, which is as general feature of II–VI compounds [40]. It is worthy to be noted that the band gap as estimated in the present work is underestimated if one compares the result with the experimental. It can be justified on the basis of notion that the simple form of GGA has been considered in the present computation, which is unable to account for self-energy of the quasiparticle [41].

Figure 2 shows the density of states (DOS) for ZnS as prototype of ZnX compounds. All The DOS of other ZnX members are not given here. But DOS of ZnS is alike to that of ZnSe and ZnTe.

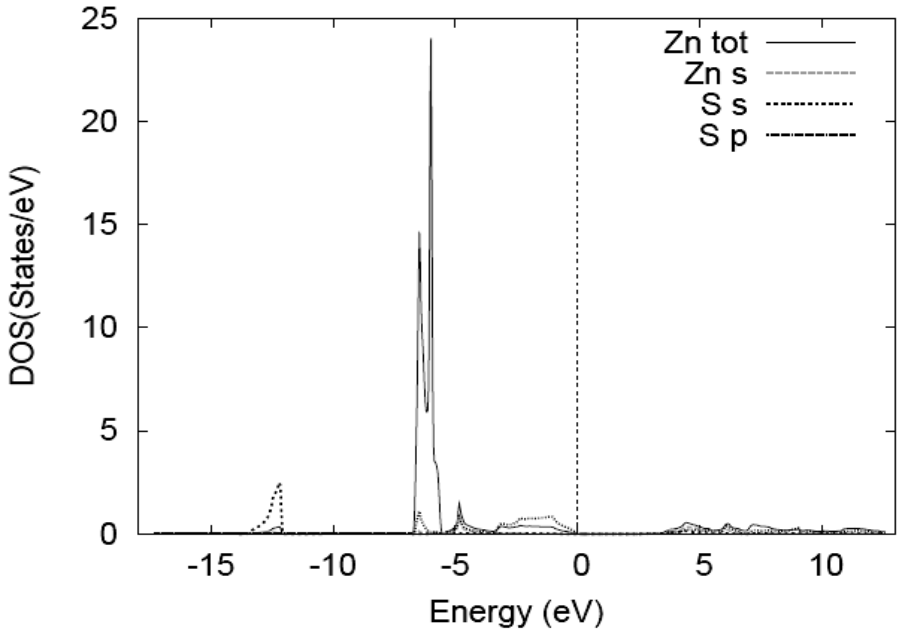

Figure 2: Density of states (DOS) for ZnS.

The peak height of the first structure in the total DOS is trivial and placed at -12.39 eV, -12.47 eV and -11.28 eV for X = S, Se and Te, respectively. This structure appears due to the chalcogen s states, which corresponds to the lowest positioned band with scattered in the region nearby Γ point in the reduced Brillouin zone. The next structure exists at -6.30 eV, -6.66 eV and -7.19 eV for X = S, Se and Te, respectively. The structure is an characteristic of Zn d states with specific p states of the chalcogen atoms and reside in largest number of states with smooth bands gathered between -5.7 eV and -6.6 eV in ZnS. A smaller amount of dispersion of such bands consequences in severe peaks. An extensive spread in DOS is found in the energy range of -5.7 eV and zero energy for ZnX compounds. The peaks in this energy range appear from the chalcogen p states partly mixed with Zn s states and they affect the upper Valence Band. If one move to higher energy or more precisely above the Fermi level, the s and p states of Zn with a partial mixture of minute chalcogen d states mediate the feature in the DOS. It has been observed that the width of the valence band as estimated from the spread of the peaks in DOS distribution underneath Fermi level are 13.52 eV, 13.23 eV, 12.27 eV for X = S, Se and Te, respectively. The valence band width is minimum for ZnTe, which evidently signifies that the wave function for ZnTe is more restricted than that for ZnS.

Optical properties

The dielectric function ε(ω) can describe the interaction between photons and electrons and say about the linear response of the electron to electromagnetic radiation [42]. So the dielectric function is important for the understanding of optical properties of solids. It includes two parts, one is the imaginary part ε2(ω) and the other is real part ε1(ω). The momentum matrix is the determining factor of ε2(ω). It consists of elements emerge from the selection rules between the occupied and unoccupied states. The imaginary part ε2(ω) can be expressed as:

$$\varepsilon_2(\omega) = \frac{V e^2}{2\pi\hbar m^2 \omega^2} \int d^3k \left|\langle kn | p | kn' \rangle\right|^2 f(kn) \times \left[1 - f(kn')\right] (E_{kn} - E_{kn'} - h\omega) \quad (13)$$

ħω is the incident photon energy, p represents the momentum operator, |kn⟩ denotes the eigenfunction with eigenvalue Ekn. f(kn) represents the Fermi distribution function. The real part ε1(ω) of the dielectric function follows the Kramer–Kroning relations and can be expressed in terms of ε2(ω) as follows

$$\varepsilon_1(\omega) = 1 + \frac{2}{\pi} \int_0^{\infty} \frac{\varepsilon_2(\omega')\omega' d\omega'}{\omega'^2 - \omega^2} \quad (14)$$

The variation of the dielectric functions, ε2(ω) and ε1(ω) of ZnX as dependence on photon energy is shown in figures 3 and 4 respectively, from 0 to 14 eV incidence energy.

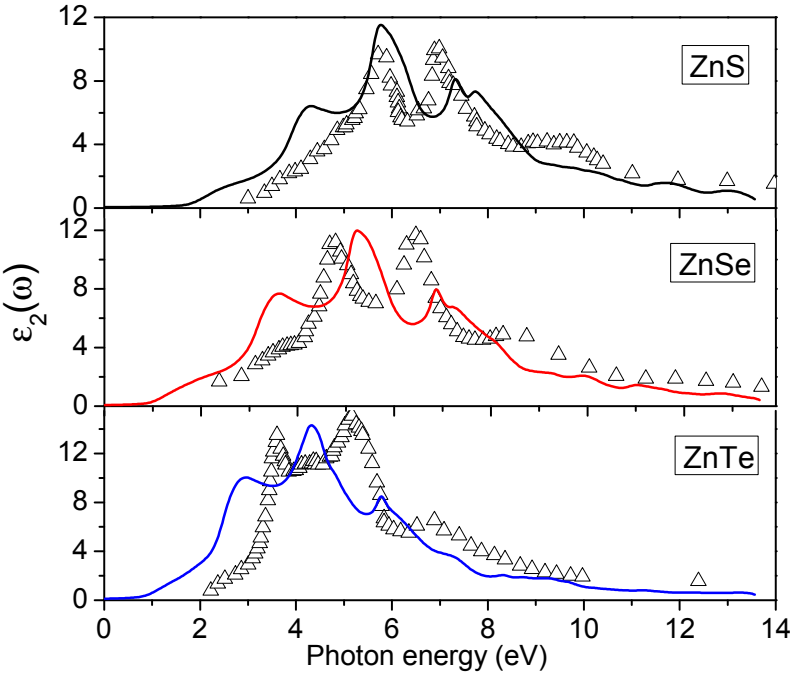

Figure 3: The variation of the imaginary part of dielectric function ($\varepsilon_2(\omega)$) as function of photon energy For ZnX compounds. (Solid line: calculated; Open triangle: experimental data from Ref. 7)

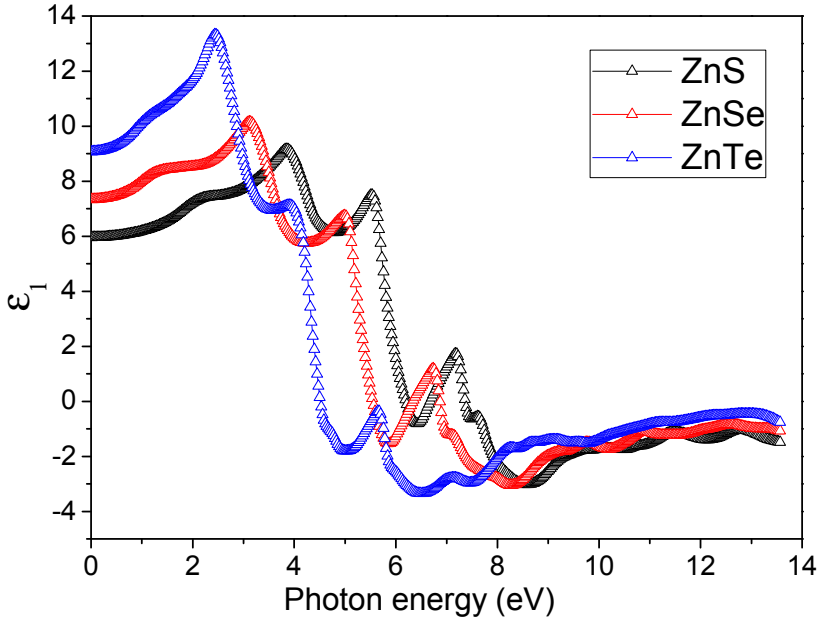

Figure 4: The variation of the real part of dielectric function ($\varepsilon_1(\omega)$) as function of photon energy for ZnX compounds.

The behavior of ε1(ω) and ε2(ω) are alike for all ZnX compounds without much differences. The main peaks of the real part of the dielectric function for ZnX occur at 3.88, 3.12, 2.44 eV for S, Se and Te respectively. The electronic contribution of the static dielectric constant occurs with the zero frequency limit ε1(0). With ascending order of chalcogenide atomic number, dielectric constant ε1(0) of the compounds are found to be 5.95, 7.34, 9.07. The imaginary part of the dielectric function ε2(ω) shows that the absorption threshold shifts slightly toward lower energy with the increase in anion atomic number. The absorption starts at about 1.55, 0.92, 0.11 eV for ZnS, ZnSe and ZnTe respectively. At these energy values, the splitting of Γv–Γc gives rise to direct optical transitions between the valence band maximum and the conduction band minimum. This is known as the fundamental absorption edge [42]. The absorption thresholds are followed by a small peak appeared at 4.35 eV, 3.55 eV and 2.98 eV in ZnS, ZnSe and ZnTe respectively due to L–L transitions. Due to the strong interband transitions between the chalcogen outermost s band and Zn 3d states, the prominent peaks occur at about 5.8, 5.2, 4.4 for ZnS, ZnSe and ZnTe, respectively. Our peak values are consistent with the experimental values [41-43].

With the knowledge of the imaginary part ε2(ω) and the real part ε1(ω) of the dielectric function, one can calculate different optical properties. The following equations are used for the calculation of energy loss function L(ω), refractive index n(ω) and reflectivity R(ω) [39–41]:

$$L(\omega) = -\mathrm{Im}\frac{1}{\varepsilon} = \frac{\varepsilon_2(\omega)}{\varepsilon_1^2(\omega) + \varepsilon_2^2(\omega)} \tag{15}$$

$$n(\omega) = \frac{1}{\sqrt{2}}\sqrt{\varepsilon_1^2(\omega) + \varepsilon_2^2(\omega) + \varepsilon_1} \tag{16}$$

$$R(\omega) = \left| \frac{\sqrt{\varepsilon(\omega)} - 1}{\sqrt{\varepsilon(\omega)} + 1} \right|^2 \quad (17)$$

The calculated optical parameters, viz., energy loss function L(ω), refractive index n(ω) and reflectivity R(ω) are shown in figures 5, 6 and 7, respectively.

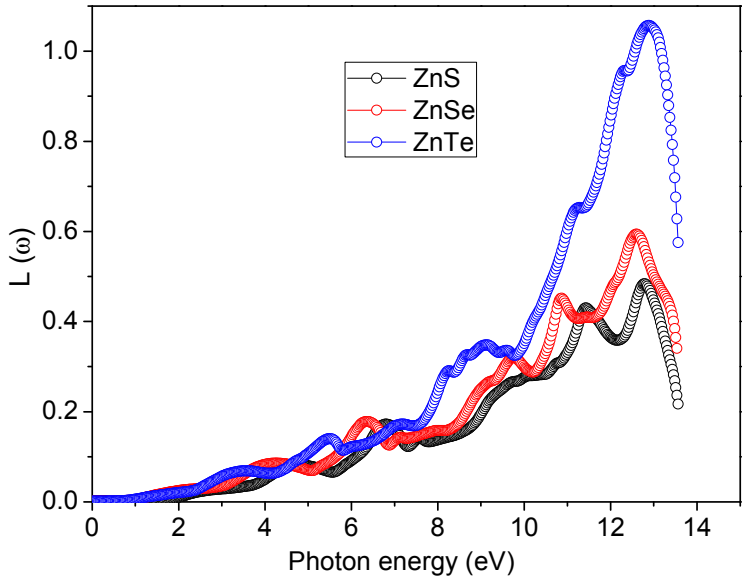

Figure 5: Variation of energy loss function (L(ω)) with photon energy for ZnX compounds.

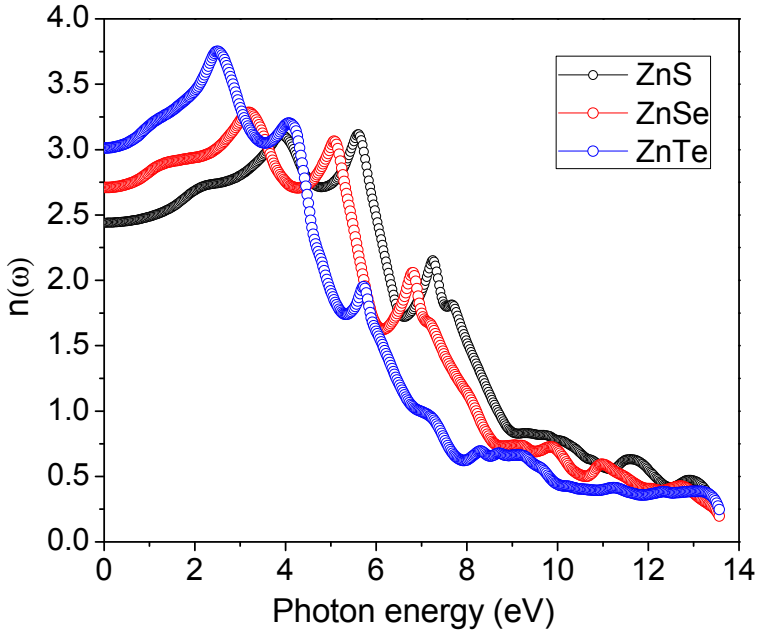

Figure 6: Variation of refractive index (n(ω)) with photon energy for ZnX compounds.

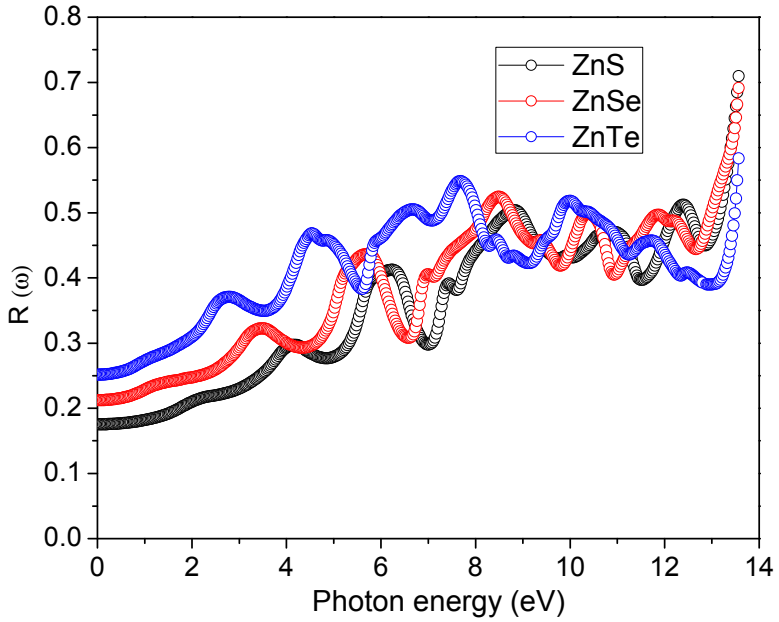

Figure 7: Variation of reflectivity R(ω) with photon energy for ZnX compounds.

L(ω) addresses the energy-loss of a fast electron navigating in the material [44]. Its highest peak corresponds to plasma frequency ωP. Usually it occurs where ε2(ω)<1, with ε1(ο) fits to the zero value [45]. The energy-loss spectra demonstrate that the principal peaks appear at 12.98, 12.81 and 12.95 eV for X = S, Se, and Te, respectively. Furthermore, while the main peaks of L(ω) are decreasing, the peaks in reflection spectra R(ω) are increasing. For instance, the sudden decrease of L(ω) takes place by 55% where the peak in R(ω) dispersion exists at 13.56eV. The reflectivity of Zn-chalcogenides keeps small value in the photon energy interval between 0 and 3.15 eV. It reveals that the compounds behaves the transmitting nature in the photon energy <3.1 eV. Also the reflectivity spectrum indicates that ZnS owns more transmitting properties than ZnTe.

IV. Conclusion

FP-LAPW + lo technique on the basis of density functional theory is used to elucidate the electronic, elastic and optical properties of Zn-chalcogenides. We obtained the structural properties such as elastic constant, mechanical parameters with the calculation based on band structure. We calculated dielectric constants, dielectric loss and refractive index. The generalized gradient approximation (GGA) was taken into consideration for the calculations of exchange and correlation effects. The results of calculations agrees well with the experimental data. The elastic constants preserve all conditions to be fulfilled for mechanical stability of the compound. The ductility in ZnX compound was detected with the increase in chalcogen atomic number. The positive Cauchy pressure (C12–C44) indicates more metallic character in their bonds. For all Zn-chalcogenides, the band structure ensures the direct energy gap at Γ point. Also with the increase in chalcogen atomic number, the absorption threshold moves to lower energy values with the increase in chalcogen atomic number. The resilient interband transitions interplay between the chalcogen outermost s state and Zn 3d states.

REFERENCES

[1] J. L. Freeouf, Phys. Rev. B 7 (1973) 3810.

[2] S. Ves, U. Schwarz, N.E. Christensen, K. Syassen, M. Cardona, Phys. Rev. B 42 (1990) 9113.

[3] M.I. Mc Mahon, R.J. Nelmes, D.R. Allan, S.A. Belmonte, T. Bovomratanaraks, Phys. Rev. Lett. 80 (1998) 5564.

[4] O. Madelung (Ed.), Numerical Data and Functional Relationship in Science and Technology, Landolt_Börnstein, New Series Group III, vol. 17, Springer-Verlag, Berlin, 1982.

[5] M. Cardona and R. Haensel, Phys. Rev. B 1 (1970) 2605.

[6] A. E. Merad, M. B. Kanoun, G. Merad, J. Cibert, and H. Aourag, Mater. Chem. Phys. 92 (2005) 333.

[7] Optical Constants of Crystalline and Amorphous Semiconductors: Numerical Data and Graphical Information, edited by S. Adachi (Kluwer Academic, Boston, 1999).

[8] R. Klucker, H. Nelkowski, Y. S. Park, M. Skibowski, and T. S. Wagner, Phys. Status Solidi B 45 (1971) 265.

[9] P. Hohenberg and W. Kohn, Phys. Rev. 136 (1964) B864.

[10] W. Kohn and L. J. Sham, Phys. Rev. 140, A (1965) 1133.

[11] R. Laskowski and N. E. Christensen, Phys. Rev. B 73 (2006) 045201.

[12] S. Z. Karazhanov, P. Ravindran, U. Grossner, A. Kjekshus, H. Fjellvåg, and B. G. Svensson, J. Appl. Phys. 100 (2006) 043709.

[13] S. Z. Karazhanov, P. Ravindran, U. Grossner, A. Kjekshus, H. Fjellvåg, and B. G. Svensson, J. Cryst. Growth 287 (2006) 162.

[14] W. R. L. Lambrecht, A. V. Rodina, S. Limpijumnong, B. Segall, and B. K. Meyer, Phys. Rev. B 65 (2002) 075207.

[15] L. C. Lew Yan Voon, M. Willatzen, M. Cardona, and N. E. Christensen, Phys. Rev. B 53 (1996) 10703.

[16] M.-Z. Huang, W.Y. Ching, Phys. Rev. B 47 (1993) 9464.

[17] G. K. H. Madsen, P. Plaha, K. Schwarz, E. Sjöstedt, L. Nordström, Phys. Rev. B 64 (2001) 195134.

[18] K. Schwarz, P. Blaha, G. K. H. Madsen, Comput. Phys. Commun. 147 (2002) 71.

[19] J.P. Perdew, K. Burke, M. Ernzerhof, Phys. Rev. Lett. 77 (1996) 3865

[20] F. D. Murnaghan, Proc. Natl. Acad. Sci. USA. 30 (1944) 382.

[21] H. J. Monkhorst, J. D. Pack, Phys. Rev. B. 13 (1976) 5188.

[22] P. Blaha, K. Schwarz, G.K.H. Madsen, D. Kvasnicka, J. Luitz, WIEN2k, An augmented plane wave plus local orbitals program for calculating crystal properties, Vienna University of Technology, Austria, 2001.

[23] B.H. Lee, J. Appl. Phys. 41 (1970) 2988.

[24] A. S. Verma, B. K. Sarkar and V. K. Jindal, Pramana 74 (2010) 851.

[25] M. Moakafi, R. Khenata, A. Bouhemadou, F. Semari, A. H. Reshak, M. Rabah, Comput. Mater. Sci. 46 (2009) 1051.

[26] F. Kalarasse, L. Kalarasse, B. Bennecer, A. Mellouki, Comp. Mat. Sci. 47 (2010) 869.

[27] S. F. Pugh, Philosophical Magazine 45 (1954) 823.

[28] S. Ganeshan, S. L. Shang, H. Zhang, Y. Wang, M. Mantina, Z. K. Liu, Intermetallics 17 (2009) 313.

[29] Z. Sun, S. Li, R. Ahuja, J. M. Schneide, Solid State Commun. 129 (2004) 589.

[30] P. Wachter, M. Filzmoser, J. Rebizant, Physica B 293 (2001) 199.

[31] C. Jansiukiewicz, V. Karpus, Solid State Commun. 128 (2003) 167.
[32] S. Adachi, T. Taguchi, Phys. Rev. B. 43 (1991) 9569.
[33] N. E. Christensen, O. B. Christensen, Phys. Rev. B. 33 (1986) 4739.
[34] E. D. Ghahramani, D. J. Moss, J. E. Sipe, Phys. Rev. B. 43 (1991) 9700.
[35] G.-D. Lee, M. H. Lee, J. Ihm, Phys. Rev. B. 52 (1995) 1459.
[36] S.-H. Wei, A. Zunger, Phys. Rev. B. 53 (1996) R10457.
[37] S. N. Rashkeev, W. R. L. Lambrecht, Phys. Rev. B. 63 (2001) 165212.
[38] Jian Sun, Hui-Tian Wang, Nai-Ben Ming, Julong He, Yongjun Tian, Appl. Phys. Lett. 84 (2004) 4544.
[39] Y. Shen, Z. Zhou, J. Appl. Phys. 103 (2008) 074113.
[40] M. Dadsetani, A. Pourghazi, Phys. Rev. B 73 (2006) 195102.
[41] F. Wooten, Optical Properties of Solids, Academic, New York, 1972.
[42] R. Khenata, A. Bouhemadou, M. Sahnoun, A. H. Reshak, H. Baltache, M. Rabah, Comput. Mater. Sci. 38 (2006) 29.
[43] L. Hannachi, N. Bouarissa, Superlattices Microstruct. 44 (2008) 794.
[44] A. Bouhemadou, R. Khenata, Comput. Mater. Sci. 39 (2007) 803.
[45] R. Saniz, L.H. Ye, T. Shishidou, A.J. Freeman, Phys. Rev. B 74 (2006) 014209